FERMILAB-CONF-09-262-AD

MEASUREMENT AND SIMULATION OF SPACE CHARGE EFFECTS IN A MULTI-BEAM ELETRON BUNCH FROM AN RF PHOTOINJECTOR*

M. M. Rihaoui[1,2], P. Piot[1,3], J. G. Power[2], Z. Yusof[2] and W. Gai[2]
[1] Department of Physics, Northern Illinois University DeKalb, IL 60115
[2] High Energy Physics Division, Argonne National Laboratory, Argonne, IL 60439, USA
[3] Accelerator Physics Center, Fermi National Accelerator Laboratory, Batavia, IL 60510, USA

Abstract

We report on a new experimental study of the space charge effect in a space-charge-dominated multi-beam electron bunch. A 5 MeV electron bunch, consisting of a variable number of beamlets separated transversely, was generated in a photoinjector and propagated in a drift space. The collective interaction of these beamlets was studied for different experimental conditions. The experiment allowed the exploration of space charge effects and its comparison with three-dimensional particle-in-cell simulations. Our observations also suggest the possible use of a multi-beam configuration to tailor the transverse distribution of an electron beam.

INTRODUCTION

Several theoretical and experimental studies have previously addressed detrimental effects due to an inhomogeneous initial distribution in a rf photoinjector, e.g., photocathode drive laser transverse distribution non-uniformities. In most investigations, the beam is statistically characterized using its rms properties. For instance Ref. [3] experimentally explores the impact of transverse modulation on the root-mean-square (rms) transverse emittance. Although this is a universal characterization relying on the concept of "equivalent beam" [4, 5] important details of the beam evolution might be missed. The pioneering work of Reiser and co-workers underlined the importance of studying the evolution of the beams transverse distribution and not only its rms properties [6, 7]. Our experiment used a quincunx pattern to generate five beamlets separated transversely. In this Paper, we present a similar experiment performed in an rf photoinjector using a ~ 5 MeV bunched electron beam. Masking the transverse distribution of the photocathode drive-laser allowed the generation of a beam that consisted of several beamlets separated transversely. The evolution of the beamlets transverse density provides information on transverse space charge effects which are validated against particle-in-cell (PIC) simulations. Furthermore, our experimental observations hint to a possible use of multi-beamlet configuration to transversely control a beam. This could open new ways of manipulating an electron beam using space charge interaction between several beams in a photoinjector. Several schemes based on space charge interaction have been proposed as ways to control or shape charged-particle beams. For instance Ref. [8] discusses the design of a very fast kicker based on such a scheme.

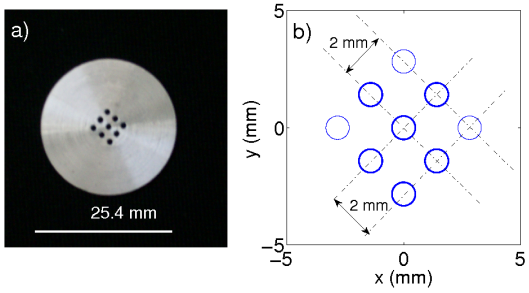

Figure 1: Picture (a) of the aluminum mask used to shape the laser beam into a series of transversely-separated beamlets and corresponding closeup of the mask geometry (b). In the experiments reported in this paper only five or six holes were not obstructed [show as thicker line circles in (b)] and the mask was oriented to yield the pattern shown in (b) on the virtual photocathode [see also Fig. 2 (left image) for the corresponding uv laser transverse density].

EXPERIMENTAL SETUP

The experiment was performed at the Argonne Wakefield Accelerator (AWA) [9]; see Ref. [10] for a detailed description of the facility. The transverse distribution of the electron bunch produced in a 1-1/2 cell rf-gun was transversely tailored by controlling the transverse distribution of the uv photocathode drive laser. The laser was intercepted by an aluminum mask consisting of a series of identical holes that could be selectively blocked (see Fig. 1). The mask's center-to-center hole separation is 2 mm and the hole diameter is 1 mm. The uv laser beam temporal profile was measured with a streak camera and can be approximated by a Gaussian distribution with rms duration of $\sigma_t \simeq 2$ ps. The transverse size of the photoemitted electron beam is controlled by a solenoid (referred to as L3). A YAG screen (referred to as YAG1) located 3.36 m downstream of the photocathode provides a measurement of the transverse beam density. The charge is measured using an integrated current monitor located at the rf gun exit.

*The work of M.R. and P.P. is supported by the US Department of Energy under Contract DE-FG02-08ER41532 with Northern Illinois University. W.G., J.P., and Z.Y. are supported by the U.S. Department of Energy under Contract No. DE-AC02-06CH11357 with Argonne National Laboratory.

LOW CHARGE REGIME

The operating conditions of the main subsystems of the photoinjector, used during the experiment reported herein, are gathered in Table 1. The first experiment consisted in generating a low charge electron beam comprising six beamlets (Fig. 2) arranged in an asymmetric pattern. This enabled us to identify the orientation of the pattern on both the virtual cathode and YAG1. Due to low space charge effects, the beamlets do not interact strongly and effectively behave as independent macroparticles. The observed pattern rotation between the photocathode and YAG1 , visible in Fig. 2 results from the Larmor precession induced as the beam propagates through the L3 magnetic lens. The rotation angle is given by [11]: $\theta(z) = \int_0^z [eB(r=0,z)]/[2m\gamma(z)\beta(z)c]dz$ where $B(r=0,z)$ is the axial component of magnetic field experienced by the beam, $\gamma(z)$ the beam's Lorentz factor and $\beta(z) \equiv [1-\gamma(z)^{-2}]^{1/2}$. The rotation angle downstream of the solenoid field, $\theta(\infty)$,was calculated by numerically integrating the latter equation using the axial magnetic field obtained from POISSON [12] while $\beta(z)$ was computed with IMPACT-T [13]. The calculated rotation angle downstream of the solenoidal field was found to be $\theta(\infty) = -32 \pm 2$ deg (the quoted uncertainty comes from the uncertainty on the peak E-field in the rf gun). The computed value compares well with the measured roration angle of $\theta(\infty) = -34.7 \pm 2.6$ deg for a peak axial magnetic field $\hat{B} = 0.339$ T.

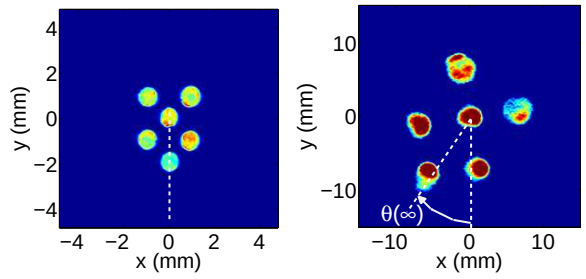

Figure 2: (Color) False color image of the measured uv laser transverse distribution on the virtual cathode (VC) location (left) and corresponding measured electron beam distribution at YAG1 location (right). The charge is $Q = 20 \pm 2$ pC.

To aid in understanding the experiment, we performed 3D PIC simulations of the beam dynamics using the program IMPACT-T. The code uses the electrostatic space charge routine where the force is found by solving Poissons equation in the bunch's rest frame [13]. IMPACT-T was run with a simplex optimizer [14] to fine tune the operating parameters of the accelerator used in the model to match the low charge measurements. During the optimization process the E-field on the cathode, laser injection phase and L3 peak axial B-field, $\hat{B}$, were varied to insure the simulation of a low charge quincunx pattern reproduces the low charge measurement on YAG1 [shown in Fig. 3 (left column)]. The minimization criterion for the optimization was to match the measured and simulated positions of the beamlets' centroid. The set of parameters obtained are compiled in Table 1 and are in good agreement with the settings inferred from the accelerator control system.

Table 1: Nominal accelerator settings during the experiment. The "Experiment" and "Model" columns respectively correspond to values inferred from the AWA control system and values obtained when matching the Impact-T model to the single-particle-dynamics measurements.

Parameter (unit)	Experiment	Model
Laser rms duration (ps)	1.9 ± 0.2	1.9
Laser phase (deg)	50 ± 5	53
Gun E-field (MV/m)	54 ± 3	51
L3 peak B-field (T)	$[0.30, 0.40]$	[0.30,0.40]
High charge (nC)	0.9 ± 0.1	0.9
Low charge (nC)	0.015 ± 0.005	0.015
Kinetic Energy (MeV)	5.20 ± 0.10	5.28

HIGH CHARGE REGIME

When the charge per bunch is increased to 1 nC space charge become significant resulting in (1) a change in beamlet intra-dynamics and (2) in interactions between the beamlets. Such interactions result in the development of unexpected features that depend on the initial pattern, especially the appearance of tails.

In Fig. 3 we consider an initial quincunx pattern and

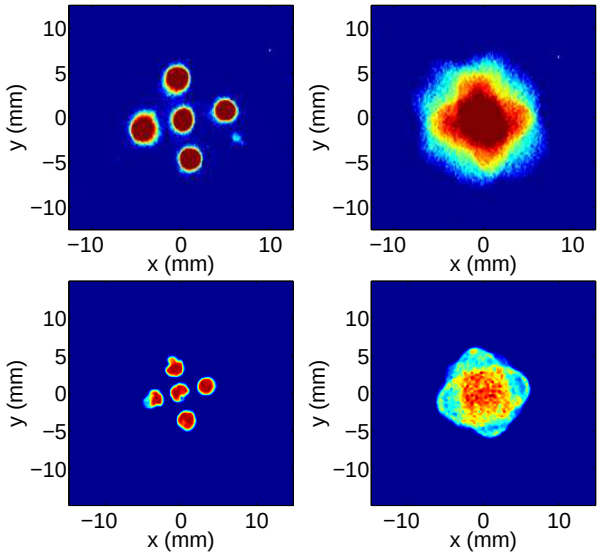

Figure 3: (Color) False color image of measured (top row) and simulated (bottom row) beam density at YAG1 for the low (left) and high (right) charge case with $\hat{B} \simeq 0.35$ T

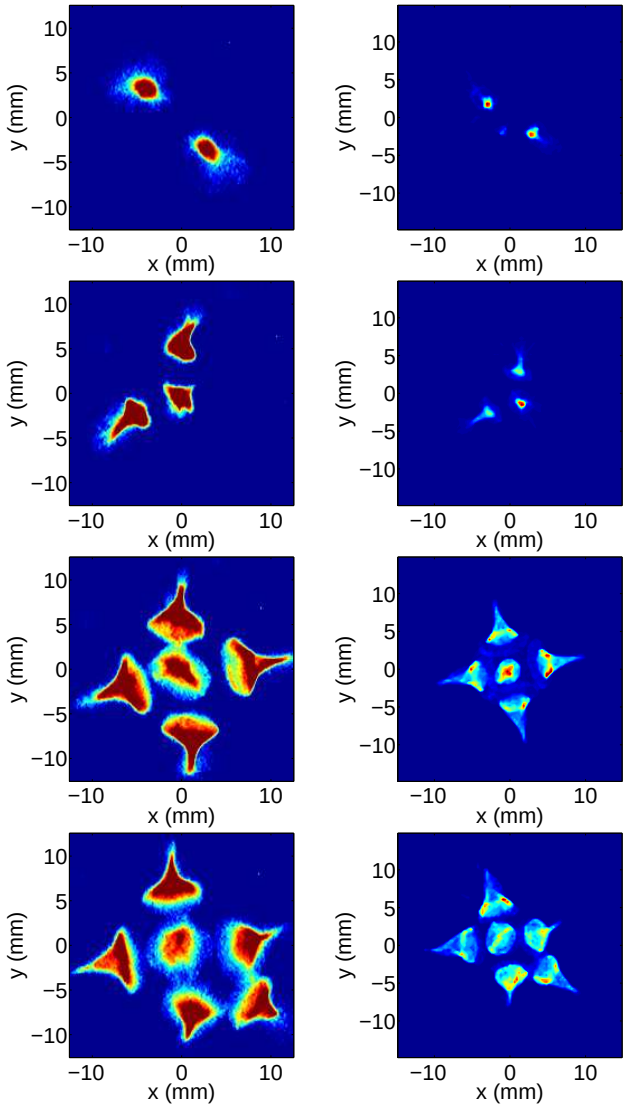

Figure 4: (Color) False color image of the measured (left column) and simulated (right) distribution on YAG1 for a two, three, five, and six (from to to bottom) initial beamlet pattern. The L3 peak B-field is $\hat{B} \simeq 0.37$ T.

compared the measured and simulated density distributions at the YAG1 location for the low and high charge cases (left and right column respectively). Increasing the strength of the solenoid leads to the appearance of tails on the peripheral beamlets; see Ref. [10]. In Fig. 4 we show similar measurements and simulations for different initial patterns for $\hat{B} = 0.37$ T. For this setting of the solenoid the beamlets develop tails pointing outward from the barycenter of the charge distribution.

An analysis, described in Ref. [10], discussed the origin of the tail formation observed on some of the pictures. We initially attributed the formation of tails to the crossing over of the beamlets (as the $\hat{B}$ is increased). However using IMPACT-T we found that the effect was caused by the space charge interaction at the early stage of the bunch generation and transport. In particular the non-cylindrical symmetry of the distribution lead to a stronger space charge induced defocusing effect for the population in the outer region of the peripheral beamlets than for the ones in the inner region. While in the rf gun, the beamlets overlap (see Ref. [10]) and the resulting potential exhibits local minima which results in weaker defocussing forces along certain directions (that depends on the symmetry fold of the distribution). Eventually the beamlets crossover (at approximately $z = 130$ cm from the photocathode for $\hat{B} = 0.37$ T) and separate (starting at $z = 150$ cm). The central beamlet acquires a shape impressed by the overall symmetry of the multi-beam pattern. The main cause for the largely defocused radial tail containing the inner population of the peripheral beamlets is the transverse force produced at the early stage of the beam transport.

POSSIBLE APPLICATIONS

Although in the experiment discussed herein we used an external focusing element, a magnetic lens, to force the beamlets trajectories to cross each other and effectively result in the focusing of the central beamlet, one could, in principle, specially design a photoinjector system without an external focusing element. Similarly, using other configurations of surrounding beamlets, one could possibly provide a means for tailoring the bunch transverse distribution. The technique discussed here might be applicable to electron sources based on superconducting rf guns, where the use of an external magnetic field to focus (or shape) the beam can be difficult. Finally, the possibility to focus a beam using a photoemitted electron beam with a temporal profile different from the main beam might also open new ways of controlling the evolution of transverse emittance associated to space-charge-dominated electron beams.

REFERENCES

[1] S. Bernal, et al., in Proc. PAC99 (New-York), 1749 (1999).

[2] J.S. Fraser, *et al.*, in Proc. PAC85 (Vancouver), 1791 (1985).

[3] F. Zhou, et al., *Phys. Rev. STAB* **5**, 094203 (2002).

[4] C. Lejeune and J. Aubert, *Adv. Electron. Electron Phys. Suppl.* **A 13**, 159 (1980).

[5] F. R. Sacherrer, *IEEE Trans. Nucl. Sci.*, **NS-18**, 1105 (1971).

[6] M. Reiser *et al.*, *Phys. Rev. Lett.* **61**, 2933 (1988).

[7] I. Haber, *et al.*, Phys. Rev. A. **44**, 8 (1991).

[8] V. Shiltsev, *Nucl. Intrum. Method*, **A 374**, 137 (1996).

[9] See `http://gate.hep.anl.gov/awa`.

[10] M. Rihaoui, et al., preprint FNAL-PUB-08-507APC (2008).

[11] M. Reiser *The Theory and design of Charged Particle Beams*, Wiley series in beam physics and accelerator technology, Edited by John Wiley & Sons, Inc. (1994).

[12] J. H. Billen *et al.*, in Proc. PAC93 (Washington DC), 790 (1993).

[13] J. Qiang, et al., *Phys. Rev. STAB* **9**, 044204 (2006).

[14] H. Shang, *et al*, in Proc. PAC05 (Knoxville), 4230 (2005).